Roughness and Scaling Properties of Oxide Glass Surfaces at the Nanoscale

Zhen Zhang,[1,2] Simona Ispas,[1] and Walter Kob[1,*]
[1]*Laboratoire Charles Coulomb (L2C), University of Montpellier and CNRS, F-34095 Montpellier, France*
[2]*Center for Alloy Innovation and Design, State Key Laboratory for Mechanical Behavior of Materials, Xi'an Jiaotong University, Xi'an 710049, China*

(Received 14 July 2020; accepted 22 January 2021; published 12 February 2021)

Using atomistic computer simulations we determine the roughness and topographical features of melt-formed (MS) and fracture surfaces (FS) of oxide glasses. We find that the topography of the MS is described well by the frozen capillary wave theory. The FS are significant rougher than the MS and depend strongly on glass composition. The height-height correlation function for the FS shows an unexpected logarithmic dependence on distance, in contrast to the power law found in experiments. We unravel the crucial role of spatial resolution on surface measurements and conclude that on length scales less than 10 nm FS are not self-affine fractals.

DOI: 10.1103/PhysRevLett.126.066101

The roughness of surfaces plays a crucial role for the functional properties of a material, including friction [1,2], adhesion [3], catalytic activity [4,5], and transport properties [6]. Understanding the nature of this roughness and modifying it is thus of great practical importance. In comparison to the surfaces of crystalline materials, the surfaces of amorphous materials such as glasses have received much less attention since the disorder renders the probing and characterization of such systems difficult [7–12]. Since a glass is an out-of-equilibrium system, the properties of its surface depend on the process by which it has been produced. Usually two types of pristine (i.e., without postprocessing) glass surfaces are considered: (i) Melt-formed surfaces (MS) that result from cooling a liquid with a free surface to the solid state and (ii) Fracture surfaces (FS), resulting from a mechanical failure.

The topography of a MS is often described using the concept of a frozen liquid interface [13,14], i.e., upon cooling the sample, the capillary waves of the surface freeze at a temperature T_0. Thus the roughness of a pristine MS is predicted to be $\sigma = \sqrt{k_B T_0/\gamma}$, where σ is the standard deviation of the surface height fluctuation, k_B is Boltzmann's constant, and γ is the surface tension at T_0. Atomic force microscope (AFM) experiments on oxide glass surfaces have shown that this prediction works well if one uses for T_0 the glass transition temperature [15–17]. This theoretical approach also predicts that the height-height correlation function

$$\Delta z(r) = \sqrt{\langle [z(r+x) - z(r)]^2 \rangle_x}, \qquad (1)$$

which gives the height difference between two points separated by a distance r along a direction x, increases like $(\Delta z)^2 \propto \ln r$. This logarithmic dependence has been validated experimentally with r ranging from around 10 to 1000 nm [15]. However, for $r < 10$ nm the dependence on r is basically unknown.

In contrast to the case of the MS, obtaining a reliable description of the topography of the FS is very challenging since the latter results from a highly nonlinear process which involves a complex interplay between heterogeneities in the composition, microstructure, and mechanical properties of the glass (see, e.g., Refs. [18–20] for reviews). Experimental studies of oxide glasses have shown that the roughness of the FS depends strongly on the composition [16,21,22] and is larger than the one found in MS [16]. AFM measurements have given evidence that the FS of various materials can be described as self-affine fractals [23], i.e., the height-height correlation function scales like $\Delta z \propto r^{\zeta}$. Here ζ is the roughness (or Hurst) exponent which has been found to depend on the fracture mode, the length scale considered, and the material considered [21,22,24–26]. However, whether this self-affine description for the FS also holds down to the nanometer scale is still an open question, since at such small scales the finite size of the probing tip severely restricts the spatial resolution [27–29].

Here, using large scale atomistic simulations, we provide quantitative insight into the topographical features of oxide glasses for the length scales ranging from a few angströms to several tens of nanometers. In particular, we analyze the morphology, roughness, symmetry, and statistical scaling of the MS and FS, i.e., surfaces which have very distinct manufacturing histories.

We investigate two archetypical compositions for oxide glasses, namely, pure SiO_2 and binary Na_2O-$XSiO_2$ (denoted hereafter by NSX), with $X = 3$, 4, 5, 7, 10, and 20. The atomic interactions are described by a two-body

 © 2021 American Physical Society

effective potential (SHIK) [30,31] which has been shown to give a reliable description of the structural, mechanical, and surface properties of sodium silicate glasses [32–34]. Our samples contain typically 2.3×10^6 atoms, corresponding to box sizes of around 20 nm × 30 nm × 50 nm (in the x, y, and z directions, respectively). Periodic boundary conditions were applied in the x and y directions while in the z direction we introduced (in the melt) two free surfaces. The samples were melted and equilibrated at a high temperature (composition dependent) and then cooled down to 300 K under zero pressure. In the following we will refer to these two surfaces, generated by the melt-quench procedure, as MS. The glass samples were then subjected to an uniaxial tension with a strain rate of 0.5 ns^{-1} in the y direction until complete fracture occurred, creating thus two FS. The surface atoms were identified by using a well-established geometric method [35] which allows to study the topographical features of the surfaces. More details on the sample preparation and surface construction are given in the Supplemental Material [36].

Figure 1 shows the (color coded) height fluctuations of the surfaces for three representatives compositions: Silica, NS10 (≈9% Na_2O), and NS3 (25% Na_2O). The top and bottom panels are for the MS and FS, respectively, and the $z = 0$ level has been determined such that the mean of the fluctuations is zero. For the MS, panels (a)–(c), one recognizes that the amplitude of these height fluctuations as well as their spatial extent are basically independent of the composition. In contrast to this the FS, panels (d)–(f), show height fluctuations that are larger than the ones for the MS and clearly grow in amplitude and extent with increasing Na_2O content. Also one recognizes that the surfaces seem to be anisotropic and in the following we will quantify these observations.

Figures 2(a) and 2(b) show the distribution of the surface height z for different glass compositions. For the MS, panel (a), we find that this distribution is basically independent of the composition, in agreement with the snapshots shown in Fig. 1. In contrast to this, the distribution for the FS shows a clear dependence on the composition in that it becomes wider with increasing Na_2O concentration (i.e., smaller X). The change of the surface height distribution is directly related to the surface roughness σ, which is defined as the standard deviation of height fluctuations. Figure 2(c) shows σ as a function of the Na_2O concentration. For the MS, σ is around 0.25 nm for silica and 0.23 nm for NS3, thus showing indeed just a very mild dependence on the composition. This observation is likely related to the fact that the MS are rich in Na [34], i.e., a species that plastifies the glass, thus allowing to smooth out even small irregularities. Using the capillary wave theory mentioned above it is possible to estimate the roughness of the MS from the surface tension, and for the case of silica one finds $\sigma \approx$ 0.26 nm (data point labeled "intrinsic") [16], in very good agreement with our simulation result.

The roughness of the FS is higher than that of the MS, in agreement with the qualitative impression given by Fig. 1, and shows a clear dependence on the Na_2O content in that it increases from ≈0.42 nm for silica to ≈0.82 nm for NS3. The increase of σ with Na_2O concentration can be rationalized by the fact that, with the addition of Na, the glass becomes increasingly ductile when subjected to mechanical loading [33,47,48]. This increase of ductility originates from the enhanced heterogeneities in the

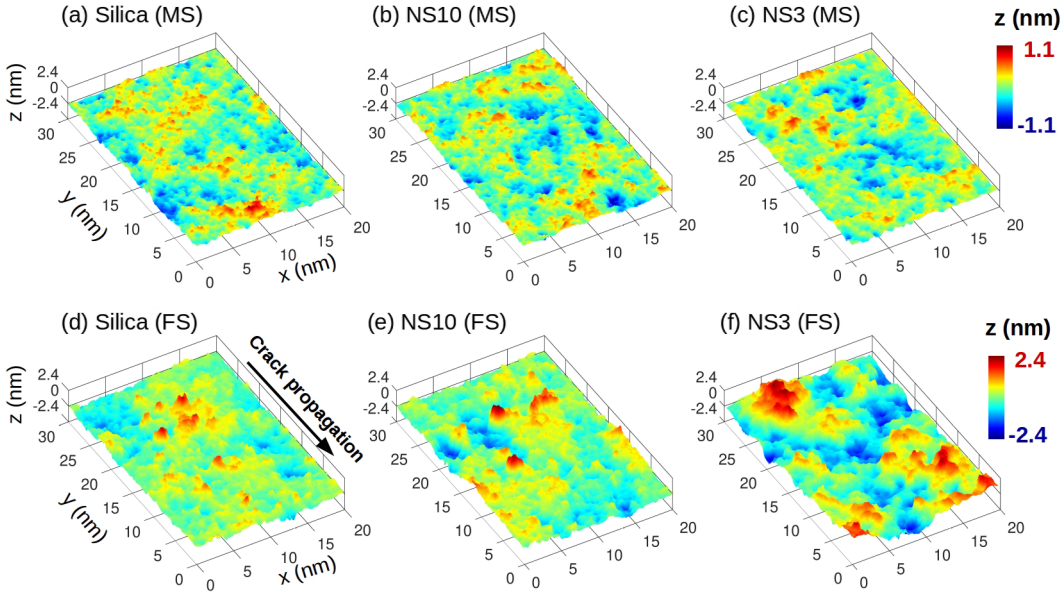

FIG. 1. Surface topography. Melt-formed surfaces (a)–(c) and fracture surfaces (d)–(f) for three representative glass compositions. For the FS, the crack propagates in the negative y direction and the crack front is parallel to the x direction. From left to right the compositions are silica, NS10, and NS3, respectively. These surfaces are shown with atomic resolution.

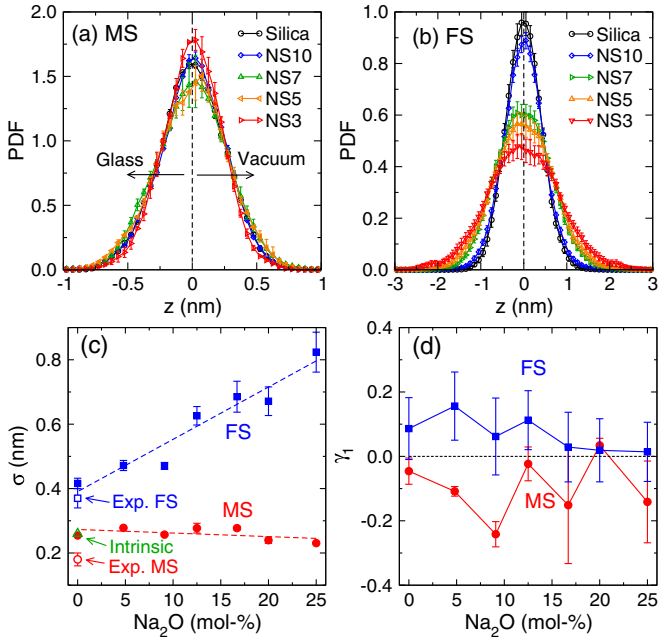

FIG. 2. Surface height distribution as a function of the composition for MS, panel (a), and FS, panel (b). The data are shown for surfaces with an area of 20 nm × 30 nm, corresponding to Fig. 1. The mean surface height $\langle z \rangle$ is equal to zero. Heights with $z > 0$ point towards the vacuum. (c) Compositional dependence of the roughness (filled symbols). The dashed lines are linear fits to the data. Experimental data are from Ref. [16]. The triangle corresponds to the intrinsic roughness of silica surface as estimated from the theory of frozen capillary waves. (d) Compositional dependence of the skewness of the surface height distribution.

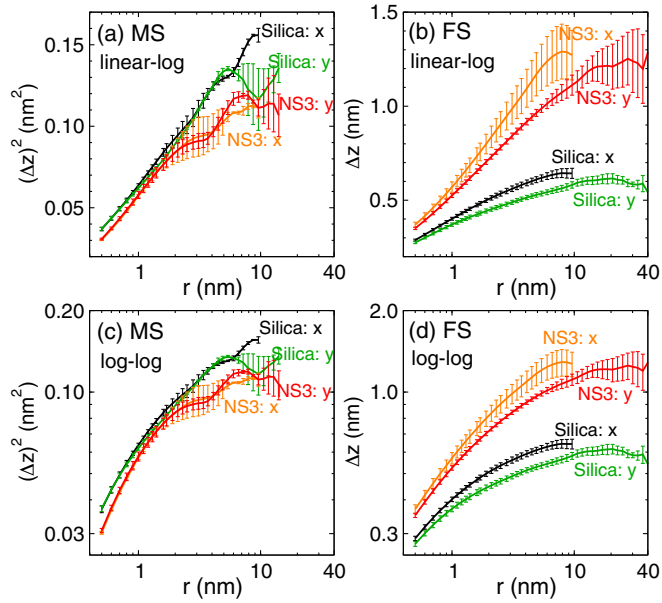

FIG. 3. Height-height correlation function (linear-log scale) for the MS (a) and FS (b). (c) and (d) Same data as in (a) and (b) but on log-log scale. Note that the ordinates for the left and right panels are not the same. The labels x and y correspond to the direction parallel to the crack front and the direction of crack propagation, respectively.

microstructure and the local plasticity of the glass, leading to a rougher fracture surface [32,49]. [Note that σ depends only weakly on the strain rate if $\dot{\epsilon} \leq 0.5\ \mathrm{ns}^{-1}$, see Fig. S1 (a) [36]].

Also included in the graph are the experimental values of the roughness for silica glass surfaces as obtained from AFM measurements [16]. One observes that these experimental data are somewhat below our simulation values and the theoretical prediction (for the MS). This discrepancy might be due to the insufficient spatial resolution of this experimental technique (see also the discussion below).

A further property of interest is the symmetry of the surfaces, which can be quantified by the skewness $\gamma_1 = \langle z^3 \rangle / (\langle z^2 \rangle)^{3/2}$ of the surface height distribution. The question of interest is whether or not the two sides of the surface (facing the vacuum or facing the glass) are statistically equivalent. Figure 2(d) shows that the MS have a negative γ_1, i.e., there are more deep holes than high protrusions, while for the FS γ_1 is positive, i.e., there are more high protrusions than deep holes. The result for the FS is coherent with the view that during the fracture process the breaking of bridges or chainlike structures gives rise to a spiky surface. Note that a nonvanishing γ_1 indicates that the capillary wave theory cannot be valid in a strict sense since this approach predicts $\gamma_1 = 0$.

To characterize the structure of the surfaces on larger scales it is useful to look at the height-height correlation function defined in Eq. (1). Figure 3(a) shows $(\Delta z)^2$ as a function of r for the MS of silica and NS3. Two (orthogonal) directions are considered and, as expected, they give the same result, indicating that the MS is isotropic. Moreover, we note that the curves for silica are slightly above the ones for NS3, indicating that the MS of silica is a bit rougher than the one of NS3, in agreement with Fig. 2(c). One also observes that $(\Delta z)^2$ increases logarithmically with r, in agreement with the prediction of the frozen capillary wave approach [13]. Since AFM experiments on MS have found the same r dependence for $r \geq 10$ nm [15], we can conclude that this theory gives a reliable description for length scales that range from the atomic (subnanometer) to the micrometer scale.

For the FS, Fig. 3(b), we find that $\Delta z(r)$ (N.B., no square) shows a linear increase with $\ln r$, thus a dependence that is very different from the one found for the MS. In this case the roughness depends on the direction in which it is measured in that the curve for the x direction (parallel to the crack front) is about 15% higher than the one for the y direction (orthogonal to the crack front), irrespective of glass composition. These results indicate that the FS is anisotropic, and its roughness depends on the composition, in agreement the experimental findings on the FS of oxide glasses [21,22,26]. Note that at large r all of the curves tend

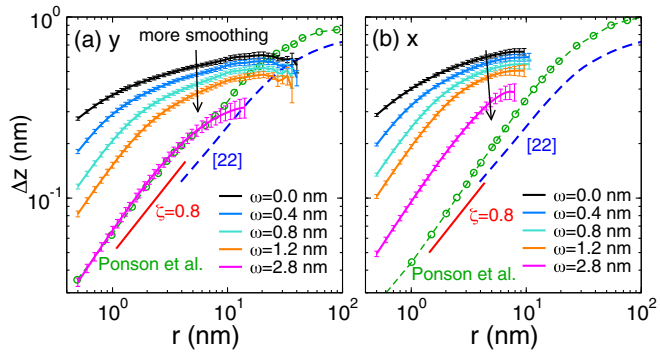

FIG. 4. Influence of spatial resolution on the surface height correlation for the FS of SiO_2. (a) and (b) The direction orthogonal and parallel to the crack front, respectively. A Gaussian filter (width ω) was applied to smooth the surface. The curves labeled $\omega = 0$ correspond to the original data. Also included are experimental data from AFM measurements of fracture surfaces produced by subcritical crack propagation [22,26].

to saturate, a behavior that is most likely related to the fact that the sample is finite and hence fluctuations are bounded. However, for small and intermediate r these finite size effects will not affect the correlation function in a significant manner and the observed scaling behavior is stable. The parameters obtained from a logarithmic fit to the small r data in panels (a) and (b), as well as for other compositions, are shown in Fig. S2. We also note that the observed scaling behaviors of the surface heights are independent of the strain rate, see Fig. S1(b).

In Figs. 3(c) and 3(d) we show on log-log scale the same data as plotted in Figs. 3(a) and 3(b), respectively. It is evident that this type of presentation of the data does not rectify it, demonstrating that on the length scales we have explored the height-height correlation is not given by a power law, i.e., neither surface has the characteristics of a fractal. We note that the $\ln r$ dependence we find for the FS is in qualitative agreement with theoretical and numerical studies on the fracture surface (generated by tensile loading) of heterogenous materials [50,51].

Our finding that the FS cannot be described as a self-affine fractal on the length scales we have considered is at odds with AFM measurements that have reported a power law dependence of $\Delta z(r)$ down to the scale of 1 nm [22,26]. To elucidate the origin of this discrepancy one has to recall that the size of an AFM tip is finite which limits the lateral resolution of the measurements [27,28] and can induce biases in the characterization of the surface [29]. In order to investigate the effect of spatial resolution we have convoluted our FS with a two-dimensional Gaussian filter [52] of width ω (see Supplemental Material [36]) and then recalculated the height-height correlation function for this smoothed surface. In Fig. 4 we show for the case of the FS of silica the resulting correlation functions for different values of ω. The curve $\omega = 0$ corresponds to the original (nonsmoothed) data. We find that with increasing ω the value of Δz decreases significantly since the convolution irons out the deep holes or high spikes. Surprisingly, we note that at small r the convoluted signal can be described well with a power law, and that the r range in which this functional form is observed increases with ω while the exponent ζ is independent of ω. For $\omega = 2.8$ nm, the correlation function of the convoluted surface in the y direction [Fig. 4(a)] matches very well the AFM data by Ponson *et al.* [26]. The exponent of the power law is $\zeta \approx 0.8$, i.e., the claimed "universal" roughness exponent found in previous experimental studies [18,22,25,26]. The data in the x direction, panel (b), shows qualitatively the same variation as the ones in the y direction. However, we find that in this case one needs to apply stronger smoothing to match quantitatively the spatial dependence of the height-height correlation of our simulated surfaces the experimental ones, a result that is related to the fact that the FS is anisotropic and the surface profile in the direction parallel to the crack front is rougher than the one in the y direction, see Fig. 3. These results indicate that the power-law observed in experiments on the scale of a few nanometers might be an artifact of insufficient resolution of the surface measurements and that in reality the correlation function takes higher values than the ones extracted from AFM studies.

In conclusion, the results of this work reveal how the topographical features of glass surfaces reflect the way they have been produced. While melt-formed surfaces can be described in a satisfactory manner by means of frozen capillary waves, surfaces originating from a fracture process exhibit a logarithmic growth of the height-height correlation, a result that so far has not been obtained from microscopic calculations.

Finally, we mention that a recent atomistic simulation study of metal-based materials (in both crystalline and amorphous forms) has found that compression-induced rough surfaces are self-affine on the length scale of 1–100 nm, a result that was attributed to atomic-scale fluctuations in plastic flow [53]. Together with our simulation results one thus can conclude that, for amorphous solids, the surface topography on small length scales depends strongly on the manufacturing history and the type of material considered. Further research exploring how material composition and the deformation mode affects the surface topography will thus be very valuable.

We thank D. Bonamy for useful discussions. Z. Z. acknowledges financial support by China Scholarship Council (NO. 201606050112). W. K. is member of the Institut Universitaire de France. This work was granted access to the HPC resources of CINES under the allocation A0050907572 and A0070907572 attributed by GENCI (Grand Equipement National de Calcul Intensif).

*Corresponding author.
walter.kob@umontpellier.fr

[1] B. N. J. Persson, O. Albohr, U. Tartaglino, A. I. Volokitin, and E. Tosatti, J. Phys. Condens. Matter **17**, R1 (2005).
[2] M. Urbakh, J. Klafter, D. Gourdon, and J. Israelachvili, Nature (London) **430**, 525 (2004).
[3] L. Pastewka and M. O. Robbins, Proc. Natl. Acad. Sci. U.S.A. **111**, 3298 (2014).
[4] M. Coppens, Catal. Today **53**, 225 (1999).
[5] A. Rimola, D. Costa, M. Sodupe, J. Lambert, and P. Ugliengo, Chem. Rev. **113**, 4216 (2013).
[6] B. Gotsmann and M. Lantz, Nat. Mater. **12**, 59 (2013).
[7] L. Hench and D. E. Clark, J. Non-Cryst. Solids **28**, 83 (1978).
[8] C. G. Pantano, Rev. Solid State Sci. **3**, 379 (1989).
[9] H. Bach, J. Non-Cryst. Solids **209**, 1 (1997).
[10] P. Bocko, P. Fenn, L. Morse, and F. Okamoto, SID 91 Digest **675** (1991).
[11] T. Dey and D. Naughton, J. Sol-Gel Sci. Technol. **77**, 1 (2016).
[12] K. Zheng, M. Kapp, and A. R. Boccaccini, Appl. Mater. Today **15**, 350 (2019).
[13] J. Jäckle and K. Kawasaki, J. Phys. Condens. Matter **7**, 4351 (1995).
[14] T. Seydel, M. Tolan, B. M. Ocko, O. H. Seeck, R. Weber, E. DiMasi, and W. Press, Phys. Rev. B **65**, 184207 (2002).
[15] T. Sarlat, A. Lelarge, E. Søndergård, and D. Vandembroucq, Eur. Phys. J. B **54**, 121 (2006).
[16] P. K. Gupta, D. Inniss, C. R. Kurkjian, and Q. Zhong, J. Non-Cryst. Solids **262**, 200 (2000).
[17] P. Roberts, F. Couny, H. Sabert, B. Mangan, D. Williams, L. Farr, M. Mason, A. Tomlinson, T. Birks, J. Knight, and P. S. Russell, Opt. Express **13**, 236 (2005).
[18] E. Bouchaud, J. Phys. Condens. Matter **9**, 4319 (1997).
[19] M. Ciccotti, J. Phys. D **42**, 214006 (2009).
[20] D. Bonamy and E. Bouchaud, Phys. Rep. **498**, 1 (2011).
[21] S. M. Wiederhorn, J. M. López-Cepero, J. Wallace, J.-P. Guin, and T. Fett, J. Non-Cryst. Solids **353**, 1582 (2007).
[22] G. Pallares, F. Lechenault, M. George, E. Bouchaud, C. Ottina, C. L. Rountree, and M. Ciccotti, J. Am. Ceram. Soc. **101**, 1279 (2018).
[23] B. B. Mandelbrot, D. E. Passoja, and A. J. Paullay, Nature (London) **308**, 721 (1984).
[24] V. Milman, N. Stelmashenko, and R. Blumenfeld, Prog. Mater. Sci. **38**, 425 (1994).
[25] C. G. Pantano, in *Current Trends in the science and technology of glass*, edited by H. Jain, A. R. Cooper, K. J. Rao, and D. Chakravorty (World Scientific, Singapore, 1989), p. 149.
[26] L. Ponson, D. Bonamy, and E. Bouchaud, Phys. Rev. Lett. **96**, 035506 (2006).
[27] F. Lechenault, G. Pallares, M. George, C. Rountree, E. Bouchaud, and M. Ciccotti, Phys. Rev. Lett. **104**, 025502 (2010).
[28] P.-E. Mazeran, L. Odoni, and J.-L. Loubet, Surf. Sci. **585**, 25 (2005).
[29] J. Schmittbuhl, J.-P. Vilotte, and S. Roux, Phys. Rev. E **51**, 131 (1995).
[30] S. Sundararaman, L. Huang, S. Ispas, and W. Kob, J. Chem. Phys. **148**, 194504 (2018).
[31] S. Sundararaman, L. Huang, S. Ispas, and W. Kob, J. Chem. Phys. **150**, 154505 (2019).
[32] Z. Zhang, PhD thesis, University of Montpellier, 2020, https://hal.archives-ouvertes.fr/tel-02902601.
[33] Z. Zhang, S. Ispas, and W. Kob, J. Non-Cryst. Solids **532**, 119895 (2020).
[34] Z. Zhang, S. Ispas, and W. Kob, J. Chem. Phys. **153**, 124503 (2020).
[35] H. Edelsbrunner and E. P. Mücke, ACM Trans. Graph. **13**, 43 (1994).
[36] See Supplemental Material at http://link.aps.org/supplemental/10.1103/PhysRevLett.126.066101 details on simulation and sample preparation, the procedure for constructing the surfaces, the influence of strain rate on surface topography, extracted parameters from the height-height correlation function, and the surface smoothing procedure, which includes Refs. [37–46].
[37] N. P. Bansal and R. H. Doremus, *Handbook of Glass Properties* (Academic Press, Orlando, 1986).
[38] S. Nosé, J. Chem. Phys. **81**, 511 (1984).
[39] W. G. Hoover, Phys. Rev. A **31**, 1695 (1985).
[40] W. G. Hoover, Phys. Rev. A **34**, 2499 (1986).
[41] S. Plimpton, J. Comput. Phys. **117**, 1 (1995).
[42] A. Stukowski, JOM **66**, 399 (2014).
[43] K. Binder and W. Kob, *Glassy Materials and Disordered Solids: An Introduction to Their Statistical Mechanics* (World Scientific, Singapore, 2011).
[44] G. N. Greaves, J. Non-Cryst. Solids **71**, 203 (1985).
[45] J. Horbach, W. Kob, and K. Binder, Phys. Rev. Lett. **88**, 125502 (2002).
[46] A. Meyer, J. Horbach, W. Kob, F. Kargl, and H. Schober, Phys. Rev. Lett. **93**, 027801 (2004).
[47] B. Wang, Y. Yu, Y. J. Lee, and M. Bauchy, Front. Mater. **2**, 11 (2015).
[48] A. Pedone, M. C. Menziani, and A. N. Cormack, J. Phys. Chem. C **119**, 25499 (2015).
[49] B. Wang, Y. Yu, M. Wang, J. C. Mauro, and M. Bauchy, Phys. Rev. B **93**, 064202 (2016).
[50] S. Ramanathan, D. Ertaş, and D. S. Fisher, Phys. Rev. Lett. **79**, 873 (1997).
[51] J. Barés, M. Barlet, C. L. Rountree, L. Barbier, and D. Bonamy, Front. Phys. **2**, 70 (2014).
[52] I. Pitas, *Digital Image Processing Algorithms and Applications* (John Wiley & Sons, New York, 2000).
[53] A. R. Hinkle, W. G. Nöhring, R. Leute, T. Junge, and L. Pastewka, Sci. Adv. **6**, eaax0847 (2020).